Interval Type-2 Fuzzy Control of Pneumatic Muscle Actuator

Xiang Huang[1], Hai-Tao Zhang[1(✉)], Dongrui Wu[1], and Lijun Zhu[2]

[1] School of Automation, State Key Laboratory of Digital Manufacturing Equipment and Technology, and the Key Laboratory of Imaging Processing and Intelligence Control, Huazhong University of Science and Technology, Wuhan 430074, China
{huangxiang92,zht,drwu}@hust.edu.cn

[2] Department of Electric and Electronic Engineering, The University of Hong Kong, Kowloon, Hong Kong, China
ljzhu@eee.hku.hk

Abstract. Pneumatic muscle actuator (PMA) is a highly nonlinear system and it is a challenging task to design the controller for it. In this paper, we aim to propose an interval type-2 fuzzy controller. Since the fuzzy sets of interval type-2 fuzzy controller are fuzzy themselves, it has better ability to deal with uncertainty than type-1 fuzzy controller. Both simulation and experiments are conducted to verify the effectiveness of the type-2 fuzzy control algorithm the results confirm that better performance can be achieved by the proposed controller.

Keywords: Pneumatic muscle actuator
Interval type-2 fuzzy control · Fuzzy membership function

1 Introduction

Pneumatic Muscle actuator (PMA), as one of modern actuation technologies, has promising applications in the field of robotics. The PMA consists of an inner nylon tube surrounded by an outer nylon braided mesh [1], and it expands and contracts as the supplying air flows in and out. In particular, when the pressure increases in PMA, it expands in radial direction and shorten in axial direction. As a result, the force is generated in the axial direction [2]. On the contrary, the PMA contracts when the internal pressure decreases and it restores to the initial state.

Compared with electric motor, PMA has advantages of high power/volume ratio, high power/mass ratio, lower price and being environment friendly. Since PMAs use the soft and flexible materials and have low stiffness, PMAs can be utilized in applications where the safety is the first priority such as in human-machine interaction scenario. Due to these advantages, PMA has been widely used in robotics [3–6].

Supported by National Natural Science Foundation of China with Grant No. U1713203.

Z. Chen et al. (Eds.): ICIRA 2018, LNAI 10984, pp. 423–431, 2018.
https://doi.org/10.1007/978-3-319-97586-3_38

The PMA system is a highly nonlinear system, therefore accurate modeling and control are very difficult. In recent years, efforts have been devoted to the modeling and control of PMAs. PID control is the most frequently used method [7], due to its simple structure. However a PMA is time-varying dynamical system, a simple PID control can not always guarantee a good performance. Various types of controllers were proposed to improve the performance, e.g., adaptive controller [8], neural network controller [9,10], sliding mode controller [11,12], mode predictive controller [13,14] etc.

Fuzzy controllers [15–17] are proposed to deal with system uncertainties. Most of these fuzzy controllers utilized Type-1 fuzzy controllers, but it is less capability to deal with uncertainties [18,19] than type-2 fuzzy controller. In this paper, an interval type-2 fuzzy controller is designed to control PMAs where the fuzzy membership functions are intervals. We carry out the simulation and experiment comparison between type-1 fuzzy controller and the proposed type-2 fuzzy controller, showing that the latter can achieve better performance.

The remainder of this paper is organized as follow. Section 2 presents the model of the PMA and introduces the control objective. In Sect. 3, the type-2 fuzzy controller is constructed. Both simulation and experiments on PMA systems are conducted in Sect. 4 to show the effectiveness of proposed controller. In Sect. 5, conclusions are finally drawn.

2 Modeling of PMA

Pneumatic muscles (PMs) are regarded as a combination of nonlinear elastic, viscous and contractile elements [2], and the dynamics can be represented as follows

$$M\ddot{X} + B\dot{X} + KX = F - Mg \tag{1}$$

where M is the mass of the load and X is the displacement of the PMA. The elastic coefficient B, viscous coefficient K and contractile force F are pressure-dependent and given as follows.

$$\begin{aligned} B &= b_1 P + b_2 \\ K &= k_1 P + k_2 \\ F &= f_1 P + f_2 \end{aligned} \tag{2}$$

where b_1, b_2, k_1, k_2, f_1 and f_2 are coefficients that might be time-varying. The schematic model is illustrated in Fig. 1.

In order to move the PM in two direction, an initial pressure P_0 is supplied such that the PM rests at $X = x_0$. According to (1), one has

$$(k_1 P_0 + k_2)x_0 = f_1 P_0 + f_2 - Mg \tag{3}$$

Let $P = P_0 + u$ and $X = x_0 + x_d$ where u is pressure increment from initial pressure P_0 and x_d is the corresponding displacement increment. With the change of variable and (3), dynamics (1) becomes

$$M\ddot{x}_d = -(b_1 P_0 + b_2)\dot{x}_d - (k_1 P_0 + k_2)x_d + (f_1 - k_1 x_0 - k_1 x_d - k_1 \dot{x}_d)u \tag{4}$$

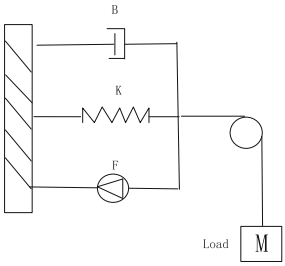

Fig. 1. Reynolds' model for a PMA.

Let $x = [x_d, \dot{x}_d]^T$, Eq. (4) can be rewritten as

$$\begin{aligned} \dot{x} &= Ax + B(x)u \\ y &= Cx \end{aligned} \tag{5}$$

with $A = \begin{bmatrix} 0 & 1 \\ -(k_1P_0 + k_2)/M & -(b_1P_0 + b_2)/M \end{bmatrix}$, $B(x) = [0, (f_1 - k_1x_0 - k_1x_d - b_1\dot{x}_d)/M]^T$, $C = [1, 0]$. Then, the objective of the tracking problem is to design the controller u for a given reference signal r such that

$$\begin{aligned} \lim_{t\to\infty} e_1(t) &= x_d(t) - r(t) = 0 \\ \lim_{t\to\infty} e_2(t) &= \dot{x}_d(t) - \dot{r}(t) = 0 \end{aligned} \tag{6}$$

where $\dot{e}_1(t) = e_2(t)$. Let $e = [e_1, e_2]^T$, the state-space for error is given as

$$\dot{e} = A_e e + B_e(r, e)u + G(r, \dot{r}, \ddot{r}) \tag{7}$$

where $A_e = A$, $B_e(r, e) = [0, (f_1 - k_1x_0 - k_1(r + e_1) - b_1(\dot{r} + e_2))/M]^T$, $G(r, \dot{r}, \ddot{r}) = [0, (-(k_1P_0 + k_2)r - (b_1P_0 + b_2)\dot{r} - \ddot{r})/M]^T$.

3 Controller Design

As illustrated in Fig. 2, the controller consists of two components

$$u = u_f + \overline{u} \tag{8}$$

where u_f is an interval type-2 fuzzy feedback controller and $\overline{u}$ is feedforward controller compensating for $G(r, \dot{r}, \ddot{r})$ at steady state, i.e., $B_z(r, 0)\overline{u} = -G(r, \dot{r}, \ddot{r})$. Note that at steady state ((6) is achieved), one has

$$\overline{u} = \frac{\ddot{r} + (b_1P_0 + b_2)\dot{r} + (k_1P_0 + k_2)r}{-b_1\dot{r} - k_1r + f_1 - k_1x_0}. \tag{9}$$

With Taylor series expansion, $\overline{u}_s$ can be simplified as

$$\overline{u} = \theta_1 r + \theta_2\dot{r} + \theta_3\ddot{r} \tag{10}$$

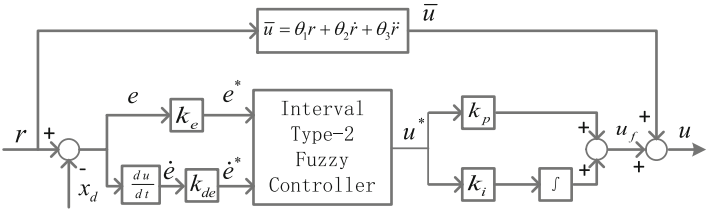

Fig. 2. The block diagram of the controller.

where $\theta_1, \theta_2, \theta_3$ are linear parameters.

For the the interval type-2 fuzzy controller, we regard $e^* = k_e e$ and $\dot{e}^* = k_{de}\dot{e}$ as the input to the fuzzy controller where k_e and k_{de} are scale factors.

Different from type-1 fuzzy membership functions (MF), every type-2 fuzzy membership function of interval type-2 controller is an interval. The membership functions (MFs) of e^* and $\dot{e}^*$ are shown in Fig. 3 where the lower bound for each membership function is determined by the parameter μ_a. Take e^* as an example (Fig. 3(a)), it combines three type-2 fuzzy membership functions, i.e., $\tilde{x}_{11}, \tilde{x}_{12}, \tilde{x}_{13}$, with corresponding shadow areas in yellow, blue and green respectively. For the membership function $\tilde{x}_{11}$, $\overline{x}_1$ is the upper bound and $\underline{x}_1$ is the lower bound. The other fuzzy sets follow in the same way. The membership functions can be written as

$$\begin{aligned}
\left[\mu_{\underline{x}_{i1}}(X), \mu_{\overline{x}_{i1}}(X)\right] &= [-\mu_a X, -X] \\
\left[\mu_{\underline{x}_{i2}}(X), \mu_{\overline{x}_{i2}}(X)\right] &= \begin{cases} [\mu_a X + \mu_a, X + 1] & (-1 \le X \le 0) \\ [-\mu_a X + \mu_a, -X + 1] & (0 \le X \le 1) \end{cases} \\
\left[\mu_{\underline{x}_{i3}}(X), \mu_{\overline{x}_{i3}}(X)\right] &= [\mu_a X, X]
\end{aligned} \tag{11}$$

with $i = 1$ for $X = e^*$ and $i = 2$ for $X = \dot{e}^*$.

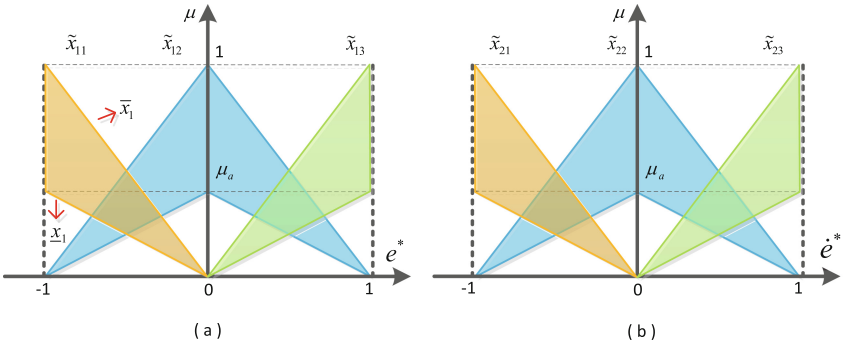

Fig. 3. (a) MFs for e^*, (b) MFs for $\dot{e}^*$. (Color figure online)

Rulebase of the proposed type-2 fuzzy controller is listed as follows:

$$
\begin{aligned}
R^1 &: \text{IF } e^* \text{ is } \tilde{x}_{11} \text{ and } \dot{e}^* \text{ is } \tilde{x}_{21}, \text{ THEN } u^* \text{ is } U_1 \\
R^2 &: \text{IF } e^* \text{ is } \tilde{x}_{11} \text{ and } \dot{e}^* \text{ is } \tilde{x}_{22}, \text{ THEN } u^* \text{ is } U_2 \\
R^3 &: \text{IF } e^* \text{ is } \tilde{x}_{11} \text{ and } \dot{e}^* \text{ is } \tilde{x}_{23}, \text{ THEN } u^* \text{ is } U_3 \\
R^4 &: \text{IF } e^* \text{ is } \tilde{x}_{12} \text{ and } \dot{e}^* \text{ is } \tilde{x}_{21}, \text{ THEN } u^* \text{ is } U_4 \\
R^5 &: \text{IF } e^* \text{ is } \tilde{x}_{12} \text{ and } \dot{e}^* \text{ is } \tilde{x}_{22}, \text{ THEN } u^* \text{ is } U_5 \\
R^6 &: \text{IF } e^* \text{ is } \tilde{x}_{12} \text{ and } \dot{e}^* \text{ is } \tilde{x}_{23}, \text{ THEN } u^* \text{ is } U_6 \\
R^7 &: \text{IF } e^* \text{ is } \tilde{x}_{13} \text{ and } \dot{e}^* \text{ is } \tilde{x}_{21}, \text{ THEN } u^* \text{ is } U_7 \\
R^8 &: \text{IF } e^* \text{ is } \tilde{x}_{13} \text{ and } \dot{e}^* \text{ is } \tilde{x}_{22}, \text{ THEN } u^* \text{ is } U_8 \\
R^9 &: \text{IF } e^* \text{ is } \tilde{x}_{13} \text{ and } \dot{e}^* \text{ is } \tilde{x}_{23}, \text{ THEN } u^* \text{ is } U_9
\end{aligned}
$$

where $U_n = [\underline{u}_n, \overline{u}_n]$. Note that we choose $\underline{u}_n = \overline{u}_n$ in this paper. U_n are given in Table 1. The firing interval for each rule is

Table 1. Rulebase for interval type-2 controller.

	$\tilde{x}_{21}$	$\tilde{x}_{22}$	$\tilde{x}_{23}$
$\tilde{x}_{11}$	$U_1 = [-1, -1]$	$U_2 = [-0.9, -0.9]$	$U_3 = [0, 0]$
$\tilde{x}_{12}$	$U_4 = [-0.9, -0.9]$	$U_5 = [0, 0]$	$U_6 = [0.9, 0.9]$
$\tilde{x}_{13}$	$U_7 = [0, 0]$	$U_8 = [0.9, 0.9]$	$U_9 = [1, 1]$

$$
F_n(e^*, \dot{e}^*) = [\underline{f}_n, \overline{f}_n] = [\mu_{\underline{x}_{1i}}(e^*) \times \mu_{\underline{x}_{2j}}(\dot{e}^*), \mu_{\overline{x}_{1i}}(e^*) \times \mu_{\overline{x}_{2j}}(\dot{e}^*)] \tag{12}
$$

where $1 \leq i \leq 3$, $1 \leq j \leq 3$, $n = 3(i-1) + j$. Compared with type-1 fuzzy controller, we also need a type-reducer. A center-of-sets type-reducer [18] is used and described as follows

$$
\begin{aligned}
u_l &= \frac{\sum_{n=1}^{L} \overline{f}_n \underline{u}_n + \sum_{n=L+1}^{N} \underline{f}_n \underline{u}_n}{\sum_{n=1}^{L} \overline{f}_n + \sum_{n=L+1}^{N} \underline{f}_n} \\
u_r &= \frac{\sum_{n=1}^{R} \underline{f}_n \overline{u}_n + \sum_{n=R+1}^{N} \overline{f}_n \overline{u}_n}{\sum_{n=1}^{R} \underline{f}_n + \sum_{n=R+1}^{N} \overline{f}_n}.
\end{aligned} \tag{13}
$$

By means of Karnik-Mendel algorithms [18], u_l and u_r can be achieved. The crisp output is finally obtained by

$$
u^* = \frac{u_l + u_r}{2} \tag{14}
$$

and u_f is

$$
u_f = k_p u^* + k_i \sum u^* \tag{15}
$$

4 Experiments

4.1 Experiment Setup

The platform for PMA experiments is shown in Fig. 4 where a Festo MAXM-20-AA type PMA is used. The air is supplied by air compressor. When the air flows in and out of PMA and causes the variation of the pressure, it results in the expansion and contraction of the PMA and thus the motion of the load attached at the end of the PMA. The displacement sensor (Firstmark NC 27622) is used to measure the displacement of moving end of the PMA. The sensor data is acquired by the A/D board of dSPACE (dSPACE 1103), and the proposed controller is executed in the dSPACE board, the voltage signal is sent to the proportional valve (Festo VPPM-6L-L-1-G18-0L6H-V1N) via the D/A board for the actuation. The proportional valve is employed to regulate the air pressure in the PMA.

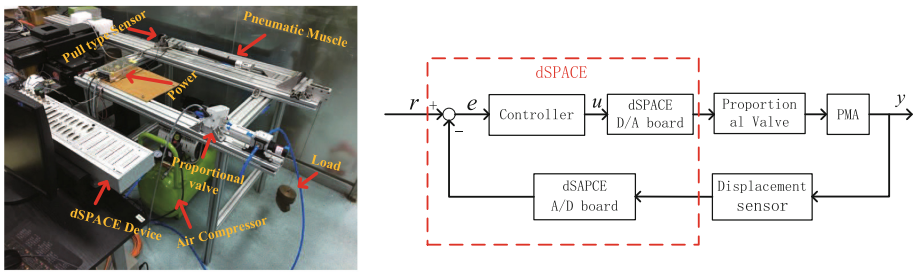

(a) (b)

Fig. 4. (a) The PMA experiment platform, (b) The block diagram of the PMA control system.

Parameters in terms B, K, F are adapted from [8] as follows

$$\begin{aligned} B &= \begin{cases} 2.2685 \times 10^{-4} P + 2435.3 & (inflation) \\ 0.0032P + 2522 & (deflation) \end{cases} \\ K &= \begin{cases} -0.2132P + 9.0638 \times 10^4 & (P \geq 32542\,\text{Pa}) \\ 0.0105P + 1.8063 \times 10^4 & (P \leq 32542\,\text{Pa}) \end{cases} \\ F &= 0.0022P - 202.32 \end{aligned} \tag{16}$$

The nominal pressure and displacement in Eq. (3) are $P_0 = 338536\,\text{Pa}$ and $x_0 = 0.2168\,\text{m}$ respectively.

4.2 Simulation

The simulation is conducted to verify the performance of proposed type-2 fuzzy controller. The tracking trajectory is a sine function

$$r(t) = 0.01 \sin(2\pi f t) \tag{17}$$

with frequency $f = 0.5\,\text{Hz}$ and amplitude $0.01\,\text{m}$.

The parameters of the controller in (8) are $k_e = 200, k_{de} = 10, k_p = 2 \times 10^4$, $k_i = 2 \times 10^6$ and $\theta_1 = 2 \times 10^3$, $\theta_2 = 3 \times 10^3$, $\theta_3 = 200$. We will vary μ_a in the fuzzy controller for the purpose of comparison, i.e., $\mu_a = 0.5$ and $\mu_a = 1$. When $\mu_a = 1$, the intervals vanish (see Fig. 3) and the controller turns out to be a type-1 fuzzy controller.

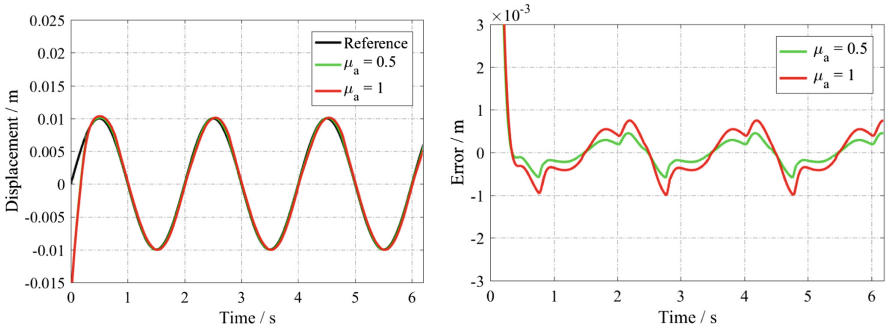

Fig. 5. Simulation results. Tracking performance comparison between the controllers with $\mu_a = 0.5$ and $\mu_a = 1$.

In Fig. 5, the performance comparison of the type-2 fuzzy controller ($\mu_a = 0.5$) and type-1 fuzzy controller ($\mu_a = 1$) are shown. Both simulations start with the same initial condition. As shown in Fig. 5, the approximated tracking can be achieved by both controllers. But it can be seen that the type-2 fuzzy controller ($\mu_a = 0.5$) can achieve better tracking performance than the type-1 fuzzy controller. The tracking error of type-2 fuzzy controller keeps at a lower level of 0.5 mm, while that of type-1 fuzzy controller nearly doubles.

4.3 Experiment Validation

In the experiment, the comparison between type-2 fuzzy controller ($\mu_a = 0.5$) and type-1 fuzzy controller ($\mu_a = 1$) is carried out. Moreover, type-2 fuzzy controller with $\mu_a = 0.4$ is added to test the influence of the parameter μ_a. Parameters for experiment are $k_e = 200$, $k_{de} = 3$, $k_p = 5 \times 10^3$, $k_i = 8 \times 10^5$ and $\theta_1 = 2 \times 10^3$, $\theta_2 = 5 \times 10^3$, $\theta_3 = 10$.

Figure 6 illustrates the tracking performances of the three controllers. For the type-2 fuzzy controller with $\mu_a = 0.4$, the maximal error reaches 4 mm. The result of the type-2 fuzzy controller with $\mu_a = 0.5$ is slightly better than that of type-1 controller with $\mu_a = 1$. The corresponding Root Mean Square Error (RMSE) for each controller is presented in Fig. 6(b). It can be conclude that the performance of type-2 fuzzy controller relies on the parameter μ_a, and the type-2 fuzzy controller with a proper μ_a achieves higher tracking accuracy than type-1 fuzzy controller.

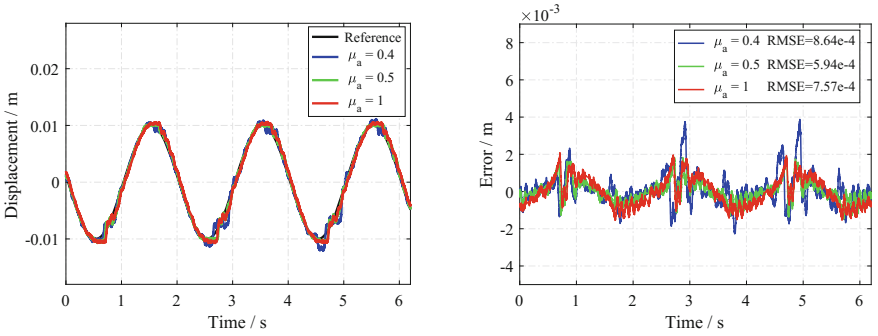

Fig. 6. Experiment results. Tracking performance comparison between controllers with $\mu_a = 0.4$, $\mu_a = 0.5$ and $\mu_a = 1$.

5 Conclusions

In this paper, an type-2 fuzzy controller is proposed. The fuzzy membership functions of the type-2 controller are intervals, which contain more expert experience and better for handling the uncertainties compared with type-1 fuzzy controller. Both simulation and experiment results illustrated the effectiveness of the proposed controller with the proper μ_a. Our further work will be focused on enriching fuzzy rules of the type-2 fuzzy controller to achieve better performance.

References

1. Caldwell, D.G., Medrano-Cerda, G.A., Goodwin, M.: Control of pneumatic muscle actuators. IEEE Control Syst. **15**(1), 40–48 (1995)
2. Reynolds, D.B., Repperger, D.W., Phillips, C.A., Bandry, G.: Modeling the dynamic characteristics of pneumatic muscle. Ann. Biomed. Eng. **31**(3), 310–317 (2003)
3. Tondu, B., Ippolito, S., Guiochet, J.: A seven-degrees-of-freedom robot-arm driven by pneumatic artificial muscles for humanoid robots. Int. J. Robot. Res. **24**(4), 257–274 (2005)
4. Ferris, D.P., Czerniecki, J.M., Hannaford, B.: An ankle-foot orthosis powered by artificial pneumatic muscles. J. Appl. Biomech. **21**(2), 189–197 (2005)
5. Hosoda, K., Sakaguchi, Y., Takayama, H., Takuma, T.: Pneumatic-driven jumping robot with anthropomorphic muscular skeleton structure. Auton. Robot. **28**(3), 307–316 (2010)
6. Rus, D., Tolley, M.T.: Design, fabrication and control of soft robots. Nature **521**(7553), 467 (2015)
7. Kawashima, K., Sasaki, T., Ohkubo, A., et al.: Application of robot arm using fiber knitted type pneumatic artificial rubber muscles. In: Proceedings of 2004 IEEE International Conference on Robotics and Automation, ICRA 2004, vol. 5, pp. 4937–4942. IEEE (2004)

8. Zhu, L., Shi, X., Chen, Z., Zhang, H.-T., Xiong, C.-H.: Adaptive servomechanism of pneumatic muscle actuators with uncertainties. IEEE Trans. Ind. Electron. **64**(4), 3329–3337 (2017)
9. Thanh, T.D.C., Ahn, K.K.: Nonlinear PID control to improve the control performance of 2 axes pneumatic artificial muscle manipulator using neural network. Mechatronics **16**(9), 577–587 (2006)
10. Jiang, X., Wang, Z., Zhang, C., Yang, L.: Fuzzy neural network control of the rehabilitation robotic arm driven by pneumatic muscles. Ind. Robot Int. J. **42**(1), 36–43 (2015)
11. Aschemann, H., Schindele, D.: Sliding-mode control of a high-speed linear axis driven by pneumatic muscle actuators. IEEE Trans. Ind. Electron. **55**(11), 3855–3864 (2008)
12. Jouppila, V.T., Gadsden, S., Bone, G.M., et al.: Sliding mode control of a pneumatic muscle actuator system with a pwm strategy. Int. J. Fluid Power **15**(1), 19–31 (2014)
13. Schindele, D., Aschemann, H.: Nonlinear model predictive control of a high-speed linear axis driven by pneumatic muscles. In: American Control Conference, 2008, pp. 3017–3022. IEEE (2008)
14. Bone, G.M., Xue, M., Flett, J.: Position control of hybrid pneumatic-electric actuators using discrete-valued model-predictive control. Mechatronics **25**, 1–10 (2015)
15. Chan, S.W., Lilly, J.H., Repperger, D.W., Berlin, J.E.: Fuzzy PD+I learning control for a pneumatic muscle. In: The 12th IEEE International Conference on Fuzzy Systems, FUZZ 2003, vol. 1, pp. 278–283. IEEE (2003)
16. Chang, M.K.: An adaptive self-organizing fuzzy sliding mode controller for a 2-DOF rehabilitation robot actuated by pneumatic muscle actuators. Control Eng. Pract. **18**(1), 13–22 (2010)
17. Xie, S.Q., Jamwal, P.J.: An iterative fuzzy controller for pneumatic muscle driven rehabilitation robot. Expert Syst. Appl. **38**(7), 8128–8137 (2011)
18. Mendel, J.M.: Uncertain Rule-Based Fuzzy Logic Systems: Introduction and New Directions. Prentice Hall PTR, Upper Saddle River (2001)
19. Wu, D.: A brief tutorial on interval type-2 fuzzy sets and systems. Fuzzy Sets Syst. (2010)